

## Personalized schedules for biopsies in prostate cancer patients

John Author\*, Jane Author, and Dick Author

Department of Statistics, University of Latex, Coventry CV4 7AL, U.K

\**email*: author@address.edu

**SUMMARY:** Low risk prostate cancer patients enrolled in active surveillance (AS) programs have to undergo biopsies on a frequent basis for examination of disease progression. Majority of the AS programs worldwide employ fixed schedules of biopsies for all patients. It has been found that such fixed and frequent schedules discourage to receive biopsies, and also bring a financial burden on the healthcare systems. Motivated by the world's largest AS program PRIAS, in this paper we present personalized schedules for biopsies to counter these problems. Using joint models for time to event and longitudinal data, our methods combine information from previous biopsy results and historical prostate-specific antigen (PSA) levels of a patient, to schedule the next biopsy. Lastly, we present criteria to compare the efficacy of personalized schedules with that of existing biopsy schedules, and a method to select the optimal schedule.

**KEY WORDS:** Personalized medicine; Prostate cancer; Active surveillance; Joint models.

### 1. Introduction

In this decade prostate cancer is the second most frequently diagnosed cancer (14% of all cancers) in males worldwide (Torre et al., 2015), and the most frequent (19% of all cancers in USA alone) in economically developed countries (Siegel, Miller, and Jemal, 2017). The increase in diagnosis of low grade prostate cancers has been attributed to increase in life expectancy and increase in number of screening programs (Potosky et al., 1995). A major issue of screening programs that also has been established in other types of cancers (e.g. breast cancer) is over-diagnosis. To avoid overtreatment, patients diagnosed with low grade prostate cancer are often motivated to join active surveillance (AS) programs. The goal of AS is to routinely examine the progression of prostate cancer and avoid serious treatments such as surgery or chemotherapy as long as they are not needed.

Currently the largest AS program worldwide is Prostate Cancer Research International Active Surveillance (PRIAS) (Bokhorst et al., 2015). Patients enrolled in PRIAS are closely monitored using serum prostate-specific antigen (PSA) levels, digital rectal examination (DRE) and repeat prostate biopsies. Results from biopsies are graded on a scale called Gleason, which takes values between 2 and 10, with 10 corresponding to a serious state of the disease. At the time of induction in PRIAS, patients must have a Gleason score of 6 or less, DRE score of cT2c or less and a PSA of 10 ng/mL or less. In PRIAS a PSA doubling time (PSA-DT), measured as the inverse of the slope of regression line through the base 2 logarithm of PSA values, of less than 3 years indicates of prostate cancer progression. However until either DRE or Gleason are observed to be higher than the aforementioned thresholds, patients are not removed from AS for curative treatment (Bokhorst et al., 2016). When the Gleason score becomes greater than 6, it is also known as Gleason reclassification (referred to as GR hereafter).

Biopsies are reliable but they are also difficult to conduct, cause pain and have serious side effects such as hematuria and sepsis (Loeb et al., 2013). Due to these reasons majority of the AS programs worldwide strongly adhere to not having more than 1 biopsy per year. Performing a biopsy annually (we refer to it as annual schedule hereafter) has the advantage that GR can be detected within 1 year of its occurrence. The drawbacks of annual schedule although, are not only medical but also financial. Keegan et al. (2012) have shown that annual schedules can cost more than the treatment (brachytherapy or prostatectomy) to AS programs, and if biopsies were to be conducted every other year, then up to 28% increase in savings from AS over treatment could be achieved per head. Despite this, several AS programs employ the annual schedule (Tosoian et al., 2011; Welty et al., 2015).

The PRIAS schedule is less rigorous than annual schedule and yet it has a high non-compliance rate for repeat biopsies Bokhorst et al. (2015). Such non-compliance reduces the effectiveness of AS programs because progression is detected late. The PRIAS schedule and compliance rates are, one biopsy each at year 1 (81%), year 4 (60%), year 7 (53%) and year 10 (33%). After year 10 biopsies are conducted every 5 years. An exception is made, if at any time a patient has PSA-DT less than 10 years, wherein annual schedule for biopsy is prescribed. When fixed schedules are prescribed to patients whose cancer progresses slowly, they often end up having unnecessary biopsies. For patients with rapidly progressing cancer, crude measures such as PSA-DT are employed to decide timing of biopsies. The fact that existing schedules require improvement is also evident in some of the reasons given by patients for non-compliance: 'patient does not want biopsy', 'PSA stable', 'complications on last biopsy' and 'no signs of disease progression on previous biopsy'.

This paper is motivated by the need to reduce the burden of biopsies and most optimally find the onset of GR (schedule for measurement of DRE is not of interest since it is a non invasive

procedure and has no serious medical implications). To this end, we intend to create schedules for biopsies which improve upon the PRIAS and annual schedule. For this purpose, one approach which stands out in particular in literature is personalized scheduling. That is, a different schedule for every patient and/or scenario. For e.g. Cost optimized personalized schedules based on Markov models have been proposed by Bebu and Lachin (2017). Cost optimized personalized equi-spaced screening intervals, using Microsimulation Screening Analysis (MISCAN) models have been proposed by OMahony et al. (2015). Parmigiani (1998) have used information theory to come up with schedules for detecting time to event in the smallest possible time interval. Most of these methods however create an entire schedule in advance. In contrast Rizopoulos et al. (2016) have proposed dynamic personalized schedules for longitudinal biomarkers using the framework of joint models for time to event and longitudinal data (Tsiatis and Davidian, 2004; Rizopoulos, 2012).

The schedules we propose in this paper are tailored separately for every patient, and are dynamic. That is, biopsies are scheduled at different time points per patient utilizing his available PSA measurements and previous biopsy results up to that point in time. We achieve this using joint models. Based on these models we obtain a full specification of the joint distribution of the PSA levels and time of GR. We further use it to define a patient-specific posterior predictive distribution of the time of GR given the observed PSA measurements and previous biopsies. Using the general framework of Bayesian decision theory, we propose a set of loss functions which are minimized to find the optimal time of performing a biopsy. These loss functions yield us two categories of personalized schedules, those based on expected time of GR and those based on the risk of GR. We also analyze an approach where the two types of schedules are combined. To compare the proposed personalized schedules with the PRIAS and annual schedule we conduct a simulation study, and then discuss various metrics for evaluating the efficacy of each schedule, and a method to choose the most suitable one.

The role of PSA measurements in personalized schedules is important, because PSA measurements are easy to obtain, and consequently they are cost effective. The PSA measurement process does not lead to any side effects and thus compliance rate for measurement of PSA levels is high (91% in PRIAS). Most importantly, it was found in PRIAS that PSA-DT was indicative of GR (Bokhorst et al., 2015). The information from PSA was however not fully utilized. More specifically, when PSA was observed to be stable, patients/doctors in PRIAS not always complied with the biopsy schedule. In this regard, the usage of joint models allows more sophisticated modeling of PSA levels and information from repeat biopsies than PRIAS, and thus offers a more informative decision making process.

The rest of the paper is organized as follows. Section 2 covers briefly the joint modeling framework. Section 3 details the personalized scheduling approaches we have proposed in this paper. In section 4 we discuss criteria for evaluation of the efficacy of a schedule and the choice of the most optimal schedule. In Section 5 we demonstrate the functioning of personalized schedules by employing them for the patients from the PRIAS program. Lastly, in Section 6, we present

the results from a simulation study we conducted to compare personalized schedules with PRIAS and annual schedule.

## 2. Joint model for time to event and longitudinal outcomes

We start with the definition of the joint modeling framework that will be used to fit a model to the available dataset, and then to plan biopsies for future patients. Let  $T_i^*$  denote the true GR time for the  $i$ -th patient enrolled in an AS program. Let the vector of times at which biopsies are conducted for this patient be denoted by  $T_i^b = \{T_{i0}^b, T_{i1}^b, \dots, T_{iN_i^b}^b; T_{ij}^b < T_{ik}^b, \forall j < k\}$ , where  $N_i^b$  are the total number of biopsies conducted. Because of the periodical nature of biopsy schedules  $T_i^*$  cannot be observed directly and it is only known that it falls in an interval  $(l_i, r_i]$ , where  $l_i = T_{iN_i^b-1}^b, r_i = T_{iN_i^b}^b$  if the GR is observed, and  $l_i = T_{iN_i^b}^b, r_i = \infty$  if patient drops out of AS before GR is observed. Further let  $\mathbf{y}_i$  denote the  $n_i \times 1$  vector of PSA levels for the  $i$ -th patient. For a sample of  $n$  patients the observed data is denoted by  $\mathcal{D}_n = \{l_i, r_i, \mathbf{y}_i; i = 1, \dots, n\}$ .

The longitudinal outcome of interest, namely PSA level is continuous in nature and thus to model it the joint model utilizes a linear mixed effects model (LMM) of the form:

$$\begin{aligned} y_i(t) &= m_i(t) + \varepsilon_i(t) \\ &= \mathbf{x}_i^T(t)\boldsymbol{\beta} + \mathbf{z}_i^T(t)\mathbf{b}_i + \varepsilon_i(t) \end{aligned}$$

where  $\mathbf{x}_i(t)$  denotes the row vector of design matrix for fixed effects and  $\mathbf{z}_i(t)$  denotes the row vector for random effects. Correspondingly the fixed effects are denoted by  $\boldsymbol{\beta}$  and random effects by  $\mathbf{b}_i$ . The random effects are assumed to be normally distributed with mean zero and  $q \times q$  covariance matrix  $\mathbf{D}$ .  $m_i(t)$  denotes the true and unobserved value of longitudinal outcome at time  $t$ , i.e. unlike  $y_i(t)$  it is not contaminated with measurement error  $\varepsilon_i(t)$ . The error is assumed to be normally distributed with mean zero and variance  $\sigma^2$ , and is independent of the random effects  $\mathbf{b}_i$ .

To model the effect of longitudinal outcome on hazard of GR, joint models utilize a relative risk sub-model. The hazard of GR for patient  $i$  at any time point  $t$ , denoted by  $h_i(t)$ , depends on a function of subject specific linear predictor  $m_i(t)$  and/or the random effects:

$$\begin{aligned} h_i(t | \mathcal{M}_i(t), \mathbf{w}_i) &= \lim_{\Delta t \rightarrow 0} \frac{\Pr\{T_i^* \in [t, t + \Delta t) | T_i^* \geq t, \mathcal{M}_i(t), \mathbf{w}_i\}}{\Delta t} \\ &= h_0(t) \exp[\boldsymbol{\gamma}^T \mathbf{w}_i + f\{M_i(t), \mathbf{b}_i, \boldsymbol{\alpha}\}] \end{aligned}$$

where  $\mathcal{M}_i(t) = \{m_i(v), 0 \leq v \leq t\}$  denotes the history of the underlying longitudinal process up to time  $t$ .  $\mathbf{w}_i$  is a vector of baseline covariates and  $\boldsymbol{\gamma}$  are the corresponding parameters. The function  $f(\cdot)$  parametrized by vector  $\boldsymbol{\alpha}$  specifies the functional form of longitudinal outcome (Brown, 2009; Rizopoulos, 2012; Taylor et al., 2013; Rizopoulos et al., 2014; Rizopoulos, 2016) that is used in the linear predictor of the relative risk model. Some functional forms relevant to the problem at hand and their interpretation are the following:

$$\begin{cases} f\{M_i(t), \mathbf{b}_i, \boldsymbol{\alpha}\} = \alpha m_i(t) \\ f\{M_i(t), \mathbf{b}_i, \boldsymbol{\alpha}\} = \alpha_1 m_i(t) + \alpha_2 m_i'(t), \text{ with } m_i'(t) = \frac{dm_i(t)}{dt} \end{cases}$$

These formulations of  $f(\cdot)$  postulate that the hazard of GR at time  $t$  may be associated with the underlying level of the biomarker  $m_i(t)$ , or with both the level and slope of the longitudinal profile  $m'_i(t)$  at time  $t$ . Lastly,  $h_0(t)$  is the baseline hazard at time  $t$ , and is modeled flexibly using P-splines. More specifically:

$$\log h_0(t) = \gamma_{h_0,0} + \sum_{q=1}^Q \gamma_{h_0,q} B_q(t, \mathbf{v})$$

where  $B_q(t, \mathbf{v})$  denotes the  $q$ -th basis function of a B-spline with knots  $\mathbf{v} = v_1, \dots, v_Q$  and vector of spline coefficients  $\gamma_{h_0}$ . To avoid choosing the number and position of knots in the spline, a relatively high number of knots (e.g., 15 to 20) are chosen and the corresponding B-spline regression coefficients  $\gamma_{h_0}$  are penalized using a differences penalty (Eilers and Marx, 1996).

For the estimation of joint model's parameters we use a Bayesian approach. The details of the estimation method, including posterior distribution of the parameters  $p(\boldsymbol{\theta} | \mathcal{D}_n)$ , where  $\boldsymbol{\theta}$  denotes the vector of all parameters, are presented in Section 1 of the supplementary material.

### 3. Personalized schedules for repeat biopsies

Once a joint model for GR and PSA levels is obtained, the next step is to use it to create personalized schedules for biopsies. To elucidate the scheduling methods, let us assume that a personalized schedule is to be created for a new patient enumerated  $j$ , who is not present in the original sample of patients  $\mathcal{D}_n$ . Further let us assume that this patient did not have a GR at his last biopsy performed at time  $t$ , and that the PSA levels are available up to a time point  $s$ . The goal is to find the optimal time  $u \geq \max(t, s)$  of the next biopsy.

#### 3.1 Posterior predictive distribution for time to GR

Let  $\mathcal{Y}_j(s)$  denote the history of PSA levels taken up to time  $s$  for patient  $j$ . The information from PSA history and repeat biopsies is manifested by the posterior predictive distribution (referred to as PPD hereafter)  $g(T_j^*)$ , given by (conditioning on baseline covariates  $\mathbf{w}_i$  is dropped for notational simplicity hereafter):

$$\begin{aligned} g(T_j^*) &= p(T_j^* | T_j^* > t, \mathcal{Y}_j(s), \mathcal{D}_n) \\ &= \int p(T_j^* | T_j^* > t, \mathcal{Y}_j(s), \boldsymbol{\theta}) p(\boldsymbol{\theta} | \mathcal{D}_n) d\boldsymbol{\theta} \\ &= \int \int p(T_j^* | T_j^* > t, \mathbf{b}_j, \boldsymbol{\theta}) p(\mathbf{b}_j | T_j^* > t, \mathcal{Y}_j(s), \boldsymbol{\theta}) p(\boldsymbol{\theta} | \mathcal{D}_n) d\mathbf{b}_j d\boldsymbol{\theta} \end{aligned} \quad (1)$$

The posterior predictive distribution depends on the observed longitudinal history of patient  $j$  via the random effects  $\mathbf{b}_j$ . It also depends on information from the training data set  $\mathcal{D}_n$  via the posterior distribution of parameters  $p(\boldsymbol{\theta} | \mathcal{D}_n)$ .

#### 3.2 Loss functions

To find the time  $u$  of next biopsy, we use principles from statistical decision theory in a Bayesian setting (Berger, 1985; Robert, 2007). More specifically, we propose to choose future biopsy time  $u$  by minimizing the posterior expected loss

$E_g[L\{T_j^*, u\}]$ , where the expectation is taken w.r.t. the PPD  $g(T_j^*)$ . The former is given by:

$$E_g[L\{T_j^*, u\}] = \int_t^\infty L\{T_j^*, u\} p(T_j^* | T_j^* > t, \mathcal{Y}_j(s), \mathcal{D}_n) dT_j^*$$

Various loss functions  $L\{T_j^*, u\}$  have been proposed in literature (Robert, 2007). The ones we utilize, and the corresponding motivations are presented next.

**3.2.1 Expected and median time of GR.** One of the reasons, patients did not comply with the existing PRIAS schedule was 'complications on a previous biopsy'. Therefore, it makes sense to have as less biopsies as possible. In the ideal case only 1 biopsy, performed at the exact time of GR is sufficient. Hence, neither a time which overshoots the true GR time  $T_j^*$ , nor a time which undershoots is preferred. In this regard, the squared loss function  $L\{T_j^*, u\} = (T_j^* - u)^2$  and absolute loss function  $L\{T_j^*, u\} = |T_j^* - u|$  have the properties that the posterior expected loss is symmetric on both sides of  $T_j^*$ . Secondly, both loss functions have well known solutions available. The posterior expected loss for the squared loss function is given by:

$$\begin{aligned} E_g[L\{T_j^*, u\}] &= E_g[(T_j^* - u)^2] \\ &= E_g[(T_j^*)^2] + u^2 - 2uE_g[T_j^*] \end{aligned} \quad (2)$$

The posterior expected loss in (2) attains its minimum at  $u = E_g[T_j^*]$ , also known as expected time of GR. The posterior expected loss for the absolute loss function is given by:

$$\begin{aligned} E_g[L\{T_j^*, u\}] &= E_g[|T_j^* - u|] \\ &= \int_u^\infty (T_j^* - u) g(T_j^*) dT_j^* + \int_t^u (u - T_j^*) g(T_j^*) dT_j^* \end{aligned} \quad (3)$$

The posterior expected loss in (3) attains its minimum at the median of  $g(T_j^*)$ , given by  $u = \pi_j^{-1}(0.5 | t, s)$ , where  $\pi_j^{-1}(\cdot)$  is the inverse of dynamic survival probability  $\pi_j(u | t, s)$  of patient  $j$  (Rizopoulos, 2011). It is given by:

$$\pi_j(u | t, s) = \Pr\{T_j^* \geq u | T_j^* > t, \mathcal{Y}_j(s), \mathcal{D}_n\}, u \geq t \quad (4)$$

For ease of readability we denote  $\pi_j^{-1}(0.5 | t, s)$  as median $[T_j^*]$  hereafter.

**3.2.2 Dynamic risk of GR.** In a practical scenario it is possible that a doctor or a patient may not want to exceed a certain risk  $1 - \kappa$ ,  $\kappa \in [0, 1]$  of GR since the last biopsy. This could be because the cutoff  $1 - \kappa$  may differentiate between patients who will obtain GR in a given period of time, and those who will not. Or, some patients can be apprehensive about delaying biopsies beyond a certain risk cutoff. In this regard, a biopsy can be scheduled at a time point  $u$  such that the dynamic risk of GR is higher than a certain threshold  $1 - \kappa$ , beyond  $u$ . To this end, the posterior expected loss for the following multilinear loss function can be minimized to find the optimal  $u$ :

$$L_{k_1, k_2}(T_j^*, u) = \begin{cases} k_2(T_j^* - u), k_2 > 0 & \text{if } T_j^* > u \\ k_1(u - T_j^*), k_1 > 0 & \text{otherwise} \end{cases} \quad (5)$$

where  $k_1, k_2$  are constants parameterizing the loss function. The posterior expected loss  $E_g[L_{k_1, k_2}\{T_j^*, u\}]$  obtains its

minimum at  $u = \pi_j^{-1}\{k_1/(k_1 + k_2) \mid t, s\}$  (Robert, 2007). The choice of two constants  $k_1$  and  $k_2$  is equivalent to the choice of  $\kappa = k_1/(k_1 + k_2)$ .

**3.2.3 A mixed approach.** When the variance  $\text{var}_g[T_j^*]$  of  $g(T_j^*)$  is small, then  $E_g[T_j^*]$  as well as  $\text{median}[T_j^*]$  are practically very useful. However when the variance is large, there may not be a clear central tendency of the distribution. Thus a biopsy scheduled using  $E_g[T_j^*]$  or  $\text{median}[T_j^*]$  will exceed or fall short of  $T_j^*$  by a big margin. Exceeding the true GR time by a large margin can lead to grave medical consequences. In PRIAS schedule the maximum possible delay in detection of GR is 3 years. Thus we propose that if the difference between the 0.025 quantile of  $g(T_j^*)$ , and  $E_g[T_j^*]$  or  $\text{median}[T_j^*]$  is more than 3 years then proposals based on dynamic risk of GR be used instead. We call this approach a mixed approach.

### 3.3 Estimation

**3.3.1 Estimation of  $E_g[T_j^*]$  and  $\text{var}_g[T_j^*]$ .** Since there is no closed form solution available for  $E_g[T_j^*]$ , for its estimation we utilize the following relationship between expected time of GR and dynamic survival probability:

$$E_g[T_j^*] = t + \int_t^\infty \pi_j(u \mid t, s) du \quad (6)$$

There is no closed form solution available for the integral in 6 either, and hence we approximate it using Gauss-Kronrod quadrature. We preferred this approach over Monte Carlo methods to estimate  $E_g[T_j^*]$  from the PPD  $g(T_j^*)$ , because sampling directly from  $g(T_j^*)$  involved an additional step of sampling from the distribution  $p(T_j^* \mid T_j^* > t, \mathbf{b}_j, \boldsymbol{\theta})$ , as compared to the estimation of  $\pi_j(u \mid t, s)$  (Rizopoulos, 2011). The latter approach was thus computationally faster. As mentioned earlier, a limitation of  $E_g[T_j^*]$  is that it is practically useful only when the  $\text{var}_g[T_j^*]$  is small, which is given by:

$$\text{var}_g[T_j^*] = 2 \int_t^\infty (u - t) \pi_j(u \mid t, s) du - \left\{ \int_t^\infty \pi_j(u \mid t, s) du \right\}^2 \quad (7)$$

Since a closed form solution is not available for the variance expression, it is estimated similar to the estimation of  $E_g[T_j^*]$ . The variance depends both on last biopsy time  $t$  and PSA history  $\mathcal{Y}_j(s)$ . The impact of the observed information on variance is discussed in detail in Section 5.2.

**3.3.2 Estimation of  $\kappa$ .** For schedules based on dynamic risk of GR, the value of  $\kappa$  dictates the biopsy schedule and thus its choice has important consequences. In certain cases it may be chosen on the basis of doctor's advice or the amount of risk that is acceptable to the patient. For e.g. if maximum acceptable risk is 75% then  $\kappa = 0.25$ .

In cases where the choice of  $k$  cannot be based on the input of the physician or the patients, we propose to automate the choice of this threshold parameter. More specifically, we propose to choose a  $\kappa$  for which a binary classification accuracy measure (López-Ratón et al., 2014; Sokolova and Lapalme, 2009), discriminating between cases and controls, is maximized. In PRIAS, cases are patients who experience GR and the rest are controls. However, a patient can be in control

group at some time  $t$  and in the cases at some future time point  $t + \Delta t$ , and thus time dependent binary classification is more relevant. In joint models, a patient  $j$  is predicted to be a case if  $\pi_j(t + \Delta t \mid t, s) \leq \kappa$  and a control if  $\pi_j(t + \Delta t \mid t, s) > \kappa$  (Rizopoulos, 2016). The time window  $\Delta t$  can be automatically chosen as  $\arg \max_{\Delta t} AUC(t, \Delta t, s)$ , the latter being a measure of discriminative capability of the model (Rizopoulos, 2016). However such a time window may not be clinically relevant at all. In AS programs at any point in time, it is of interest to identify patients who may obtain GR in the next 1 year from those who do not, so that they can be provided immediate attention (in exceptional cases a biopsy within an year of the last one). Thus, in this work we use a  $\Delta t$  of 1 year.

In regards to automatic selection of the threshold  $\kappa$  using binary classification accuracy measures, our goal is to focus on patients whose true time of GR falls in the time window  $\Delta t$ . To this end, the measure which combines both sensitivity and precision is  $F_1$ -Score. It is defined as:

$$F_1(t, \Delta t, s) = 2 \frac{\text{TPR}(t, \Delta t, s) \text{PPV}(t, \Delta t, s)}{\text{TPR}(t, \Delta t, s) + \text{PPV}(t, \Delta t, s)}, F_1 \in [0, 1],$$

$$\text{TPR}(t, \Delta t, s) = \Pr\{\pi_j(t + \Delta t \mid t, s) \leq \kappa \mid T_j^* \epsilon(t, t + \Delta t)\},$$

$$\text{PPV}(t, \Delta t, s) = \Pr\{T_j^* \epsilon(t, t + \Delta t) \mid \pi_j(t + \Delta t \mid t, s) \leq \kappa\}$$

where  $\text{TPR}(\cdot)$  and  $\text{PPV}(\cdot)$  denote time dependent true positive rate (sensitivity) and positive predictive value (precision), the estimation for which proceeds as in Rizopoulos (2016). Since a high  $F_1$  score is desired, the optimal value of  $\kappa$  is  $\arg \max_{\kappa} F_1(t, \Delta t, s)$ .

### 3.4 Algorithm

Given the personalized scheduling methods, the next step is to iteratively create an entire schedule until GR is detected for the patient. To this end, the algorithm in Figure 3.4 elucidates the process of creating a personalized schedule for patient  $j$ . Since PRIAS and most AS programs strongly advise against conducting more than 1 biopsy per year, the algorithm adjusts the optimal time  $u$  of biopsy in case the last biopsy was performed less than an year ago.

## 4. Choosing a schedule

Given a particular schedule  $S$  of biopsies, our next goal is to evaluate the efficacy of this schedule and to compare it with other schedules. To this end, we first present the criteria for evaluation of efficacy of biopsy schedules and then discuss the choice of the optimal schedule.

### 4.1 Evaluation of efficacy of schedules

The first criteria in the evaluation of efficacy of a schedule  $S$  is the number of repeat biopsies  $N^{bS}$  it conducts before GR is detected for a patient. More specifically, our interest lies in the marginal distribution  $p(N^{bS})$  of number of biopsies for the entire population of patients. Various measures of efficacy can be extracted from this distribution, such as the mean  $E[N^{bS}]$ , or the variance  $\text{var}[N^{bS}]$ . Given the medical and financial burden associated with biopsies, a small mean and small variance is desired. Quantiles of  $p(N^{bS})$  may also be of interest. For e.g. a schedule which takes less than 2 biopsies in 95% cases may be preferred.

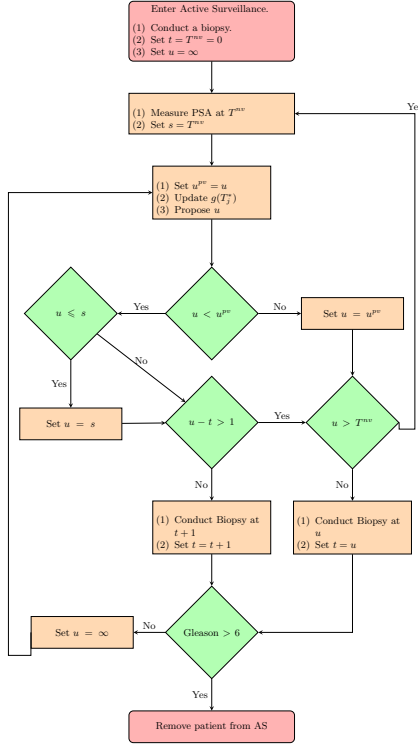


**Figure 1.** Algorithm for creating a personalized schedule for patient  $j$ .  $t$  denotes the time of the latest biopsy.  $s$  denotes the time of the latest available PSA measurement.  $u$  denotes the proposed time of personalized biopsy based on  $g(T_j^*)$ .  $u^{pv}$  denotes the time at which a repeat biopsy was proposed at the last visit to the hospital.  $T^{mv}$  denotes the time of the next visit for PSA measurement.

The second criteria in evaluation of efficacy of a schedule  $S$  is the offset. The offset for a particular patient  $j$  can be defined as  $O_j^S = T_{jN_j^{bS}}^S - T_j^*$ , where  $N_j^{bS}$  is the number of biopsies required for patient  $j$  before GR is detected and  $T_{jN_j^{bS}}^S > T_j^*$  is the time at which GR is detected. Once again the interest lies in the marginal distribution  $p(O^S)$  of the offset for the entire population of patients. A small mean  $E[O^S]$  and small variance  $\text{var}[O^S]$  are desired.

#### 4.2 Finding the most optimal schedule

Given the multiple criteria for efficacy of a schedule the next step is to find the most optimal schedule. Using principles from compound optimal designs (Läuter, 1976) we propose to choose a schedule  $S$  which minimizes the following loss function:

$$L(S) = \sum_{g=1}^G \lambda_g \mathcal{G}_g(N^{bS})^{d_g=1} \mathcal{G}_g(O^S)^{d_g=0} \quad (8)$$

where  $\mathcal{G}_g(\cdot)$  is either a function of number of biopsies or of the offset, and  $d_g$  is the corresponding indicator for this choice. Some examples of  $\mathcal{G}_g(\cdot)$  are mean, median, variance and quantile function. Constants  $\lambda_1, \dots, \lambda_G$ , where  $\lambda_g \in [0, 1]$  and  $\sum_{g=1}^G \lambda_g = 1$ , are weights to differentially weigh-in the

contribution of each of the  $G$  evaluation criteria manifested via the functions  $\mathcal{G}_g(\cdot)$ . An example loss function is:

$$L(S) = \lambda_1 E[N^{bS}] + \lambda_2 E[O^S] \quad (9)$$

Choosing values for  $\lambda_1$  and  $\lambda_2$  is not easy, because biopsies have serious medical side effects and consequently the cost of an extra biopsy cannot be quantified or compared to a unit increase in offset easily. To obviate this issue we utilize the equivalence between compound and constrained optimal designs (Cook and Wong, 1994). More specifically, it can be shown that for any  $\lambda_1$  and  $\lambda_2$  there exists a constant  $C > 0$  for which minimization of loss function in (9) is equivalent to minimization of the same, subject to the constraint that  $E[O^S] < C$ . That is, the optimal schedule is the one with the least number of biopsies and an offset less than  $C$ . The choice of  $C$  now can be based on the protocol of AS program. In the more generic case in (8), the optimal solution can be found by minimizing  $\mathcal{G}_G(\cdot)$  under the constraint  $\mathcal{G}_g < C_g; g = 1, \dots, G - 1$ .

### 5. Personalized schedules for patients in PRIAS

To demonstrate how the personalized schedules work, we apply them to the patients enrolled in PRIAS. To this end, we divide the PRIAS dataset into a training data set with 5264 patients and a demonstration dataset with 3 patients who never experienced GR. We fit a joint model to the training dataset and then use it to create personalized schedules for patients in demonstration dataset. We fit the joint model using the R package Jmbayes (Rizopoulos, 2016), which uses the Bayesian methodology to estimate the model parameters.

#### 5.1 Fitting the joint model to PRIAS dataset

The training dataset contains PSA levels and the time interval in which GR was detected, for 5264 prostate cancer patients. For every patient the following information is available: age at the time of induction, PSA at every 3 months for first 2 years and every 6 months thereafter. To detect GR, biopsies were conducted as per the PRIAS schedule (Section 1). For the longitudinal analysis of PSA we use  $\log_2$  PSA measurements instead of the raw data. This because the PSA scores take very large values around the time of disease progression, indicating that the underlying distribution for PSA is right skewed. The longitudinal sub-model of the joint model we fit is given by:

$$\log_2 \text{PSA}(t) = \beta_0 + \beta_1 (\text{Age} - 70) + \beta_2 (\text{Age} - 70)^2 + \sum_{k=1}^4 \beta_{k+2} B_k(t, \mathcal{K}) + b_{i0} + b_{i1} B_7(t, 0.1) + b_{i2} B_8(t, 0.1) + \varepsilon_i(t) \quad (10)$$

The evolution of PSA over time is modeled flexibly using B-splines. The spline for the fixed effects consists of 3 internal knots at  $\mathcal{K} = \{0.1, 0.5, 4\}$  years, and boundary knots at 0 and 7 years. The spline for the random effects consists of 1 internal knot at 0.1 years and boundary knots at 0 and 7 years. The choice of knots was based on exploratory analysis as well as on model selection criteria AIC and BIC. Age of patients was median centered to avoid numerical instabilities during parameter estimation. For the relative risk sub-model

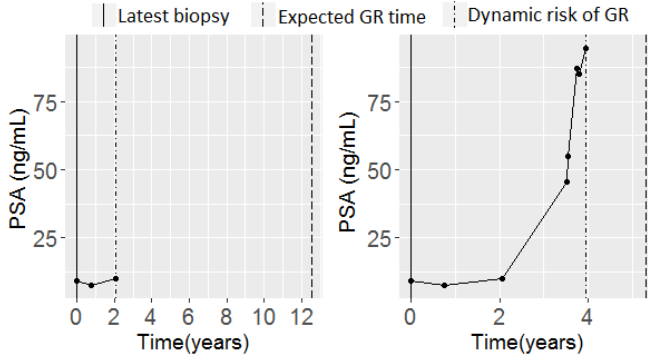


**Figure 2.** PSA and repeat biopsy history, and corresponding personalized schedules for patient 3174.

the hazard function we fit is given by:

$$h_i(t) = h_0(t) \exp [\gamma_1 \{Age - 70\} + \gamma_2 \{Age - 70\}^2 + \alpha_1 m_i(t) + \alpha_2 m'_i(t)] \quad (11)$$

where  $\alpha_1$  and  $\alpha_2$  are measures of strength of the association between hazard of GR and  $\log_2$  PSA value  $m_i(t)$  and  $\log_2$  PSA velocity  $m'_i(t)$ , respectively. Since the PRIAS schedule depends only on the observed PSA values (via PSA-DT), the interval censoring observed in PRIAS is independent and non informative of the underlying health of the patient.

From the joint model fitted to the PRIAS dataset we found that only  $\log_2$  PSA velocity was strongly associated with hazard of GR. For any patient, a unit increase in  $\log_2$  PSA velocity led to an 11 times increase in the hazard of GR. The parameter estimates for the fitted joint model are presented in detail in Section 3 of the supplementary material.

### 5.2 Demonstration of personalized schedules

Using the demonstration dataset, we next present the functioning of personalized schedules based on expected time of GR and dynamic risk of GR. The first patient of interest is patient 3174. The PPD  $g(T_j^*)$  for this patient depends only on the PSA levels since no repeat biopsies were conducted in the time period we considered. The evolution of PSA, repeat biopsy history and proposed times of biopsies are shown in Figure 2. It can be seen that the schedule of biopsy based on expected time of GR adjusts the times of biopsy according to the rise in hazard due steep rise in  $\log_2$  PSA velocity after year 2. More specifically, at 2 years the proposed biopsy time is 12.5 years whereas at 4 years it decreases to 5.3 years. A biopsy scheduled using expected time of GR at year 2 should have a larger offset  $O_j^S$  on average compared to the same at year 4. This because  $\text{var}_g[T_j^*]$  is considerably lower at year 4 as shown in Figure 3. As expected the variance also strongly depends on PSA velocity. For schedules based on dynamic risk of GR, the optimal  $1 - \kappa$  value was found to be between 0 and 0.1 at all time points. Due to the sharp rise in PSA values, this corresponds to a time very close to the time of latest biopsy (time 0). Hence the biopsies are scheduled much earlier than those based on expected time of GR.

The second patient of interest is patient 911, for whom the evolution of PSA, time of last biopsy and proposed biopsy times are shown in Figure 4. We can see the combined effect of decreasing PSA levels and a negative repeat biopsy

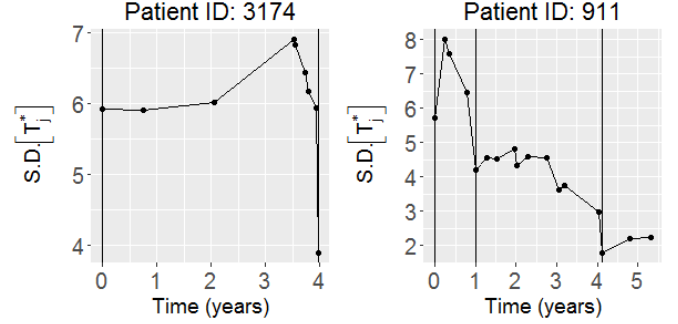


**Figure 3.** Standard deviation  $\text{S.D.}[T_j^*] = \sqrt{\text{var}_g[T_j^*]}$  over time for patient 3174 and 911. Solid vertical lines indicate biopsies.

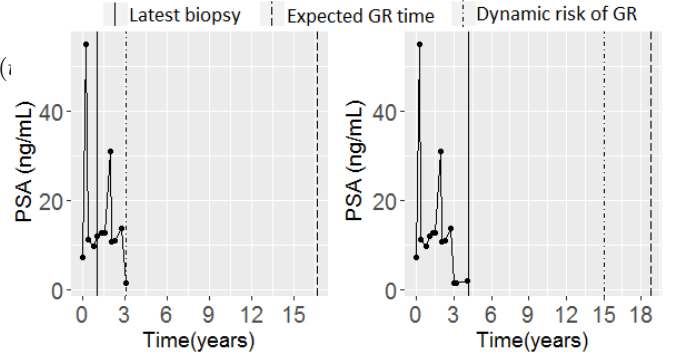


**Figure 4.** PSA and repeat biopsy history, and corresponding personalized schedules for patient 911.

on personalized schedules, between year 3 and year 4.5 for this patient. In accordance with the observed history of the patient, the proposed time of biopsy based on expected time of GR increases from 16.6 years to 18.7 years in this period. For dynamic risk of GR it increases from 3.2 years to 15 years, despite the optimal  $\kappa$  being equal to 0.98 for the entire period. We can also see that after each repeat biopsy  $\text{var}_g[T_j^*]$  decreases sharply (Figure 3), thus in turn reducing the offset as well.

Patient 2340 presents a case where information from PSA levels and repeat biopsies is conflicting. In Figure 5 we can see that the PSA for this patient becomes twice between year 2 and year 3.2. If only information from PSA is considered, then we can see that proposed time of biopsy based on expected time of GR is preponed from 12.5 years to 11.5 years during this period. However, if we also take into account the negative result from the repeat biopsy at year 2.5, then the proposed time of biopsy is postponed from 12.5 years to 15 years. The proposed time of biopsy based on dynamic risk of GR is also preponed.

## 6. Simulation study

The application of personalized schedules for patients from PRIAS demonstrated that the schedules adapt according to the historical data of each patient. However we could not perform a full scale comparison between personalized and PRIAS schedules, because the true time of GR was not known

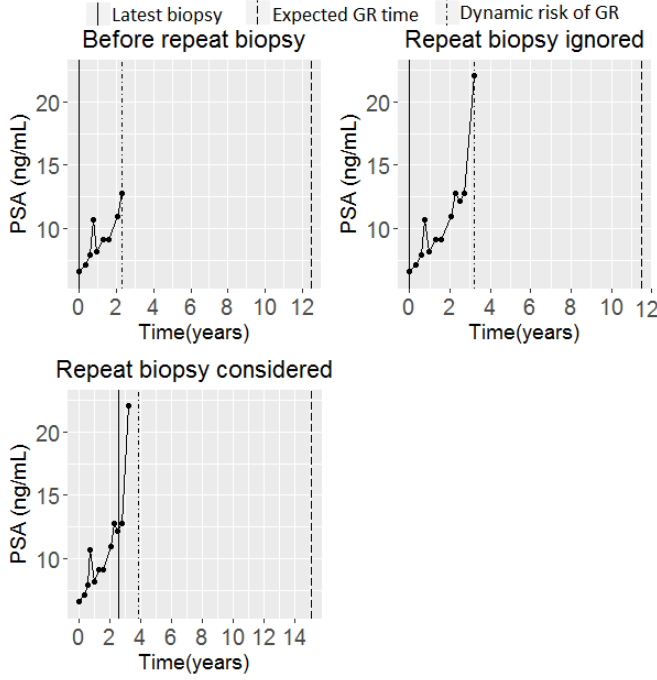


**Figure 5.** PSA and repeat biopsy history, and corresponding personalized schedules for patient 2340.

for any of the PRIAS patients. To this end, we have performed a simulation study comparing personalized schedules based on expected time of GR, median time of GR and dynamic risk of GR with a mixed approach between median time of GR and dynamic risk of GR, PRIAS schedule and annual schedule. We employ these schedules for simulated patients enrolled in a hypothetical AS program, with the same entrance criteria as PRIAS.

### 6.1 Simulation setup

**6.1.1 Patient population.** First we assume a population of patients enrolled in AS, whose PSA and hazard of GR follows a joint model of the form postulated in Section 5.1, with parameters equal to the posterior mean of parameters (CHECK WEB SUPPLEMENTARY SECTION...) estimated from the joint model fitted to PRIAS dataset. We assume that the patients in population belong to 3 equal sized subgroups  $G_1, G_2, G_3$  with different failure times. The failure times are controlled by different Weibull distributed baseline hazards for each. The shape and scale parameters  $(k, \lambda)$  for the 3 subgroups are: (1.5, 4), (3, 5) and (4.5, 6) for  $G_1, G_2$  and  $G_3$  respectively. The effect of these parameters is that the variance in GR times is highest for  $G_1$  and lowest for  $G_3$ , while the mean GR time is lowest in  $G_1$  and highest in  $G_3$ .

From the population we randomly sample a total of 408 datasets with 1000 patients each. Each dataset is split into a training (750 patients) and a test (250 patients) part. The  $k$ -th simulated training dataset  $\mathcal{D}^k$  is given by  $\mathcal{D}^k = \{l_{ki}, r_{ki}, \mathbf{y}_{ki}; i = 1, \dots, 750\}$ , where  $\mathbf{y}_{ki}$  denote the PSA measurements for the  $i$ -th patient in  $\mathcal{D}^k$ . The frequency of PSA measurements is same as that in PRIAS. Other than simulating a true GR time  $T_{ki}^*$ , we also generate a random and non-informative censoring time  $C_{ki}$ . When  $T_{ki} < C_{ki}^*$ ,

then  $l_{ki} = r_{ki} = T_{ki}^*$ , otherwise  $l_{ki} = C_{ki}$  and  $r_{ki} = \infty$ . For the test patients, censoring time is not generated.

Next we fit a joint model of the specification given in 10 and 11 to each of the  $\mathcal{D}^k, k = 1, \dots, 408$ , and obtain posterior distribution of parameters  $p(\boldsymbol{\theta} | \mathcal{D}^k)$ . Using the latter, we obtain the PPD  $g(T_{kj}^*)$  for the  $j$ -th test patient and conduct hypothetical biopsies iteratively in accordance with the algorithm in Figure 3.4.

### 6.2 Estimation

For estimation of the optimal  $\kappa = \arg \max_{\kappa} F_1(t, \Delta t, s)$ , we use a grid search approach. That is,  $F_1$  is computed using the training dataset over a fine grid of  $\kappa$  values in the interval  $[0, 1]$  and then the most optimal value is chosen.

The next step is to estimate the measures of efficacy of schedules. To this end, we estimate  $E[N^{bS}]$ ,  $\text{var}[N^{bS}]$ ,  $E[O^S]$  and  $\text{var}[O^S]$  using pooled estimates of each from the 408 test datasets, as follows:

$$\begin{aligned} E[\widehat{O^S}] &= \frac{\sum_{k=1}^{254} n_k E[\widehat{O_k^S}]}{\sum_{k=1}^{254} n_k}, \\ \text{var}[\widehat{O^S}] &= \frac{\sum_{k=1}^{254} (n_k - 1) \text{var}[\widehat{O_k^S}]}{\sum_{k=1}^{254} (n_k - 1)}, \end{aligned}$$

where  $n_k$  are the number of test patients in the  $k$ -th simulation,  $E[\widehat{O_k^S}] = \sum_{j=1}^{n_k} O_{kj}^S / n_k$  is the estimated mean and  $\text{var}[\widehat{O_k^S}] = \sum_{j=1}^{n_k} \{O_{kj}^S - E[\widehat{O_k^S}]\}^2 / (n_k - 1)$  is estimated variance of the offset for the  $k$ -th simulation. The estimates for number of biopsies  $N^{bS}$  are obtained similarly.

### 6.3 Results

From the simulations we calculated the pooled estimates of the mean and variance of number of biopsies/offset for the entire sample. The estimates are plotted in Figure 6 and also summarized in Table 1. From the figure it is evident that those schedules which conduct less biopsies on average, have a higher average offset, and vice versa. For example, the annual schedule conducts 5.2 biopsies on average, which is the highest among all schedules, however it has the least average offset of 6 months as well. On the other hand the schedule based on expected time of GR conducts only 1.9 biopsies on average, the least among all schedules but it also has the highest average offset of 15 months. The schedule based on median time of GR performs almost the same as that based on expected time of GR. As mentioned earlier the variance in number of biopsies and offset are important as well. In this regard annual schedule has the largest  $\text{var}[N^{bS}]$  since it attempts to contain the offset within an year, and consequently it has the least  $\text{var}[O^S]$ . Schedules based on expected and median time of GR perform the opposite in terms of variance.

We observe that the PRIAS schedule performs more or less the same as annual schedule. Despite this the latter may be preferred over PRIAS since it conducts only 0.38 biopsies more on average, however unlike PRIAS it has very low variance of offset, thus guaranteeing early detection for everyone. If we compare the PRIAS schedule with dynamic risk of GR based schedules, we can see that the schedule where  $\kappa$  is chosen after maximizing  $F_1$ -Score, performs better



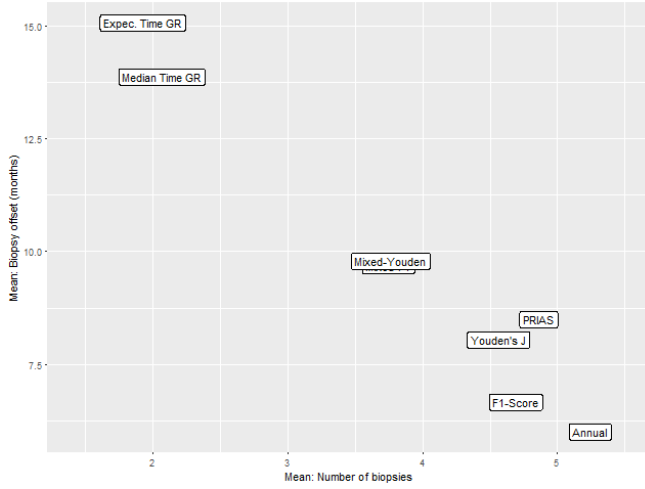


**Figure 6.** Estimated mean number of biopsies and mean offset (months) for the 7 scheduling methods using all patients. Method names are abbreviated for ease of graphing.

**Table 1**

*Pooled estimates of mean and variance of number of biopsies and offset for all patients.*

Schedule	$E[N^{bS}]$	$E[O^S]$	$\text{var}[N^{bS}]$	$\text{var}[O^S]$
Annual	5.23	6.00	6.42	11.87
PRIAS	4.85	8.46	5.52	74.22
Expected time of GR	1.92	15.06	1.42	146.31
Median time of GR	2.06	13.89	2.00	139.73
F <sub>1</sub> -Score	4.68	6.65	4.80	18.83
Mixed approach	3.76	9.74	2.88	58.35

**Table 2**

*Pooled estimates of mean and variance of number of biopsies and offset for subgroup  $G_1$ .*

Schedule	Total Patients	$E[N^{bS}]$	$E[O^S]$	$\text{var}[N^{bS}]$	$\text{var}[O^S]$
Annual	21004	4.306	6.024	9.788	11.747
PRIAS	21004	4.032	7.951	8.221	63.528
Expected time of GR	21001	1.922	15.114	1.401	149.167
Median time of GR	20937	2.068	13.87	1.999	138.896
F <sub>1</sub> -Score	21061	4.689	6.648	4.863	18.745
Mixed approach	21004	3.252	10.361	4.611	73.781

than in PRIAS schedule in all aspects. The schedule where  $\kappa$  is chosen after maximizing Youden's  $J$  has a very large  $\text{var}[O^S]$  and hence is not preferable over PRIAS. The mixed approach combines the benefits of methods with low  $E[N^{bS}]$  and  $\text{var}[N^{bS}]$ , and those methods with low  $E[O^S]$  and  $\text{var}[O^S]$ . It conducts 1.5 less biopsies than annual schedule on average and at 9.7 months the mean offset is less than an year.

We next check the performance of these methods for each of the 3 subgroups  $G_1, G_2$  and  $G_3$ . Estimates of  $E[N^{bS}]$ ,  $\text{var}[N^{bS}]$ ,  $E[O^S]$  and  $\text{var}[O^S]$  for the 3 subgroups are presented in Table 2, Table 3 and Table 4. We observe that all of the schedules which are based on personalized methods, i.e. expected time of GR, median time of GR and dynamic risk of GR based schedules perform the same across the subgroups, with trivial differences in estimates. On the other hand, the annual schedule conducts 6 biopsies on average for patients in

**Table 3**

*Pooled estimates of mean and variance of number of biopsies and offset for subgroup  $G_2$ .*

Schedule	Total Patients	$E[N^{bS}]$	$E[O^S]$	$\text{var}[N^{bS}]$
Annual	21160	5.181	5.95	4.567
PRIAS	21160	4.817	8.569	3.98
Expected time of GR	21151	1.927	15.078	1.447
Median time of GR	21189	2.062	13.947	1.994
F <sub>1</sub> -Score	21133	4.666	6.663	4.726
Mixed approach	21160	3.702	10.359	1.869

**Table 4**

*Pooled estimates of mean and variance of number of biopsies and offset for subgroup  $G_3$ .*

Schedule	Total Patients	$E[N^{bS}]$	$E[O^S]$	$\text{var}[N^{bS}]$
Annual	21222	6.214	6.03	3.118
PRIAS	21222	5.717	8.866	2.977
Expected time of GR	21234	1.921	15.006	1.375
Median time of GR	21260	2.07	13.879	2.016
Youden's $J$	21202	4.541	8.02	4.061
Mixed approach	21222	4.33	8.521	1.581

$G_3$  as compared to 4 for patients in  $G_1$ . It also has  $\text{var}[N^{bS}]$  3 times more for patients in  $G_1$  compared to  $G_3$ . This can be attributed to the former having higher variance in GR times. However for annual schedule the  $E[O^S]$  and  $\text{var}[O^S]$  remain almost the same in all groups and it always detects GR within an year of the occurrence. The PRIAS schedule differs for the 3 subgroups as well. For number of biopsies the dynamics are similar to that of annual schedule. However for offset, the PRIAS schedule has high  $E[O^S]$  and  $\text{var}[O^S]$  for patients from  $G_3$ , i.e. patients who obtain GR later. As for the mixed approach, we observe that it conducts more biopsies on average for patients from  $G_3$ , however it also has the least  $E[O^S]$ ,  $\text{var}[O^S]$  and  $\text{var}[N^{bS}]$  for the same group.

To assess the methods further, we combined data from all of the 68386 patients, and also plotted the box plots for number of biopsies and offset in Figure ?? and Figure ?? respectively. Based on the combined data, we observe that both expected and median failure time of GR based schedules have 91.7% and 92.5% of patients below offset cutoff of 36 months, respectively. They also have 80.5% and 82.3% of patients below a cutoff of 24 months. Thus they seem to be quite practical. The mixed approach offers another practically viable solution, since neither it has large  $\text{var}[N^{bS}]$ , nor  $\text{var}[O^S]$ . The estimated  $E[N^{bS}]$  is 3.8 and the estimated  $E[O^S]$  is 9.7 months. For 99.9% patients it has an offset below 36 months and for 95% patients it has an offset below 24 months. Given this offset and the fact that it conducts much less biopsies than PRIAS schedule, annual schedule, and dynamic risk of GR based schedules, it is preferable over them.

## 7. Discussion

In this paper we presented personalized biopsy scheduling methods for patients enrolled in AS programs. The problem at hand was that the AS patients have to undergo repeat biopsies frequently, which causes medical side effects and also brings financial burden. On top of that the existing schedules such



as PRIAS schedule had high patient non-compliance because of frequent biopsies and crude analysis of PSA. To approach these problems, we first came up with a joint model to combine the information from PSA as well as repeat biopsies in a more sophisticated manner than the existing PRIAS schedule. Secondly, using the information from the model, we proposed personalized schedules tailored for individual patients. We proposed 2 different class of personalized schedules: those based on central tendency of the distribution of time of GR for individual patient, and those based on dynamic risk of GR. In addition we also proposed a combination (mixed approach) of these 2 approaches. We then proposed criteria for evaluation of various scheduling methods and loss function to select the most optimal schedule.

We demonstrated using PRIAS dataset that the personalized schedules adjust the time of biopsy with results from repeat biopsies and PSA profile even when the two are not in complete concordance with each other. Secondly from the simulation study we observed that personalized scheduling method based on dynamic risk of GR ( $F_1$ -Score) performed better than PRIAS schedule in terms of both mean and variance of number of biopsies and offset. We also observed that the PRIAS schedule performed quite similar to the annual schedule and the latter may be preferred over it since the latter only conducted 0.38 biopsies more on average but it always detected GR within an year of occurrence. The schedules based on expected and median time to GR conducted only 2 biopsies on average, which is very promising compared to PRIAS and annual schedule which conducted 4.9 and 5.2 biopsies on average respectively. In addition, for schedules based on expected and median time of GR, approximately 92% of the patients had an offset less than 36 months, which is the maximum possible offset in PRIAS. If a stronger restriction is prescribed for the offset, then we propose that the mixed approach be used since it offers the best of the two worlds, i.e. not too many biopsies and not too high offset. Lastly, we observed that the personalized methods performed the same for all sub-groups in our population, however the performance of annual and PRIAS schedule was dependent on the failure times of the patients.

Although Gleason scores are susceptible to inter-observer variation (Carlson et al., 1998), we assume that any biopsy conducted after the true GR time of a patient will lead to GR detection with 100% certainty.

While each of the personalized methods has their own disadvantages and advantages, they also offer multiple choices to the AS programs to choose the one as per their requirements, instead of choosing a common fixed schedule for all patients. In this regard, there is potential to develop and analyze more personalized schedules. For e.g. using loss functions which asymmetrically penalize overshooting/undershooting the target GR time can be interesting. Another option is to choose  $\kappa$  on the basis of other binary classification accuracy measures which were not discussed in this paper. Although in this work we assumed that GR time was interval censored, in reality the Gleason scores are susceptible to inter-observer variation. Models and schedules which account for error in measurement of time of GR, will be interesting to investigate further. Lastly, there is potential for including diagnostic information from Magnetic resonance imaging (MRI) or DRE. Unlike PSA

levels such information may not always be continuous in nature, in which case our proposed methodology can be very easily extended by utilizing the framework of GLMMs in joint models.

#### ACKNOWLEDGEMENTS

The authors thank the Erasmus MC Cancer Computational Biology Center for giving access to their IT-infrastructure and software that was used for the computations and data analysis in this study.

#### SUPPLEMENTARY MATERIALS

Web Appendix A, referenced in Section 2, is available with this paper at the Biometrics website on Wiley Online Library.

#### REFERENCES

- Bebu, I. and Lachin, J. M. (2017). Optimal screening schedules for disease progression with application to diabetic retinopathy. *Biostatistics*.
- Berger, J. O. (1985). *Statistical Decision Theory and Bayesian Analysis*. Springer Science & Business Media.
- Bokhorst, L. P., Alberts, A. R., Rannikko, A., Valdagni, R., Pickles, T., Kakehi, Y., Bangma, C. H., Roobol, M. J., study group, P., et al. (2015). Compliance rates with the prostate cancer research international active surveillance (prias) protocol and disease reclassification in noncompliers. *European urology* **68**, 814–821.
- Bokhorst, L. P., Valdagni, R., Rannikko, A., Kakehi, Y., Pickles, T., Bangma, C. H., Roobol, M. J., study group, P., et al. (2016). A decade of active surveillance in the prias study: an update and evaluation of the criteria used to recommend a switch to active treatment. *European urology* **70**, 954–960.
- Brown, E. R. (2009). Assessing the association between trends in a biomarker and risk of event with an application in pediatric hiv/aids. *The annals of applied statistics* **3**, 1163–1182.
- Carlson, G. D., Calvanese, C. B., Kahane, H., and Epstein, J. I. (1998). Accuracy of biopsy gleason scores from a large uropathology laboratory: use of a diagnostic protocol to minimize observer variability. *Urology* **51**, 525–529.
- Cook, R. D. and Wong, W. K. (1994). On the equivalence of constrained and compound optimal designs. *Journal of the American Statistical Association* **89**, 687–692.
- Eilers, P. H. and Marx, B. D. (1996). Flexible smoothing with b-splines and penalties. *Statistical science* **11**, 89–121.
- Keegan, K. A., Dall’Era, M. A., Durbin-Johnson, B., and Evans, C. P. (2012). Active surveillance for prostate cancer compared with immediate treatment. *Cancer* **118**, 3512–3518.
- Läuter, E. (1976). Optimal multipurpose designs for regression models. *Mathematische Operationsforschung und Statistik* **7**, 51–68.
- Loeb, S., Vellekoop, A., Ahmed, H. U., Catto, J., Emberton, M., Nam, R., Rosario, D. J., Scattoni, V., and Lotan, Y.

- (2013). Systematic review of complications of prostate biopsy. *European urology* **64**, 876–892.
- López-Ratón, M., Rodríguez-Álvarez, M. X., Cadarso-Suárez, C., Gude-Sampedro, F., et al. (2014). Optimalcutpoints: an R package for selecting optimal cutpoints in diagnostic tests. *Journal of statistical software* **61**, 1–36.
- OMahony, J. F., van Rosmalen, J., Mushkudiani, N. A., Goudsmit, F.-W., Eijkemans, M. J., Heijnsdijk, E. A., Steyerberg, E. W., and Habbema, J. D. F. (2015). The influence of disease risk on the optimal time interval between screens for the early detection of cancer: A mathematical approach. *Medical Decision Making* **35**, 183–195.
- Parmigiani, G. (1998). Designing observation times for interval censored data. *Sankhyā: The Indian Journal of Statistics, Series A* **60**, 446–458.
- Potosky, A. L., Miller, B. A., Albertsen, P. C., and Kramer, B. S. (1995). The role of increasing detection in the rising incidence of prostate cancer. *JAMA* **273**, 548–552.
- Rizopoulos, D. (2011). Dynamic predictions and prospective accuracy in joint models for longitudinal and time-to-event data. *Biometrics* **67**, 819–829.
- Rizopoulos, D. (2012). *Joint models for longitudinal and time-to-event data: With applications in R*. CRC Press.
- Rizopoulos, D. (2016). The R package jmbayes for fitting joint models for longitudinal and time-to-event data using mcmc. *Journal of Statistical Software* **72**, 1–46.
- Rizopoulos, D., Hatfield, L. A., Carlin, B. P., and Takkenberg, J. J. (2014). Combining dynamic predictions from joint models for longitudinal and time-to-event data using bayesian model averaging. *Journal of the American Statistical Association* **109**, 1385–1397.
- Rizopoulos, D., Taylor, J. M. G., Van Rosmalen, J., Steyerberg, E. W., and Takkenberg, J. J. M. (2016). Personalized screening intervals for biomarkers using joint models for longitudinal and survival data. *Biostatistics* **17**, 149–164.
- Robert, C. (2007). *The Bayesian choice: from decision-theoretic foundations to computational implementation*. Springer Science & Business Media.
- Siegel, R. L., Miller, K. D., and Jemal, A. (2017). Cancer statistics, 2017. *CA: A Cancer Journal for Clinicians* **67**, 7–30.
- Sokolova, M. and Lapalme, G. (2009). A systematic analysis of performance measures for classification tasks. *Information Processing & Management* **45**, 427–437.
- Taylor, J. M., Park, Y., Ankerst, D. P., Proust-Lima, C., Williams, S., Kestin, L., Bae, K., Pickles, T., and Sandler, H. (2013). Real-time individual predictions of prostate cancer recurrence using joint models. *Biometrics* **69**, 206–213.
- Torre, L. A., Bray, F., Siegel, R. L., Ferlay, J., Lortet-Tieulent, J., and Jemal, A. (2015). Global cancer statistics, 2012. *CA: a cancer journal for clinicians* **65**, 87–108.
- Tosoian, J. J., Trock, B. J., Landis, P., Feng, Z., Epstein, J. I., Partin, A. W., Walsh, P. C., and Carter, H. B. (2011). Active surveillance program for prostate cancer: an update of the Johns Hopkins experience. *Journal of Clinical Oncology* **29**, 2185–2190.
- Tsiatis, A. A. and Davidian, M. (2004). Joint modeling of longitudinal and time-to-event data: an overview. *Statistica Sinica* **14**, 809–834.
- Welty, C. J., Cowan, J. E., Nguyen, H., Shinohara, K., Perez, N., Greene, K. L., Chan, J. M., Meng, M. V., Simko, J. P., Cooperberg, M. R., et al. (2015). Extended followup and risk factors for disease reclassification in a large active surveillance cohort for localized prostate cancer. *The Journal of urology* **193**, 807–811.

Received October 0000. Revised February 0000. Accepted March 0000.

## APPENDIX

### Title of appendix

Put your short appendix here. Remember, longer appendices are possible when presented as Supplementary Web Material. Please review and follow the journal policy for this material, available under Instructions for Authors at <http://www.biometrics.tibs.org>.